

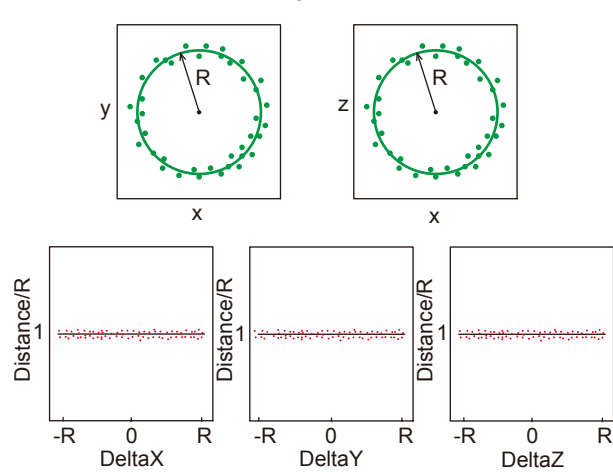
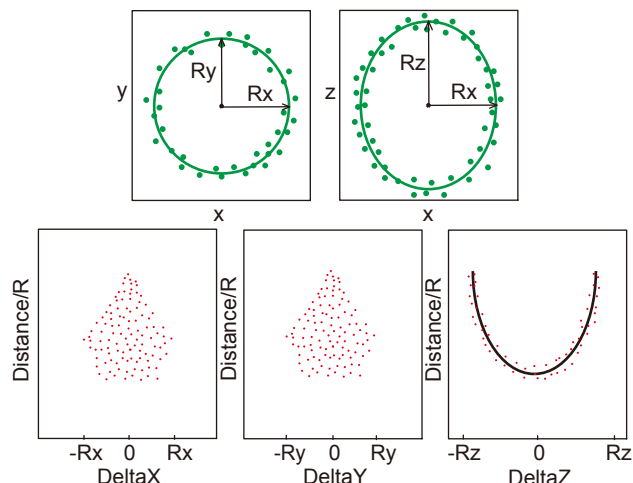
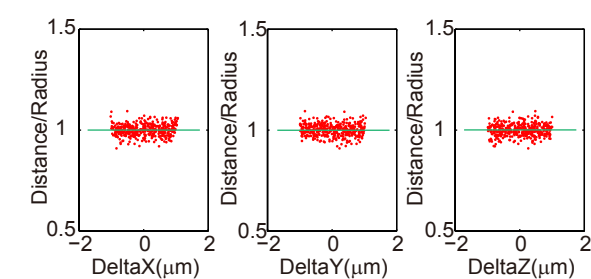
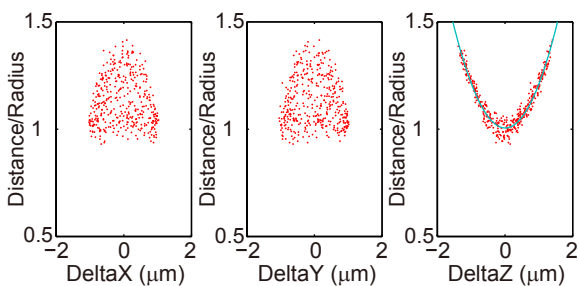
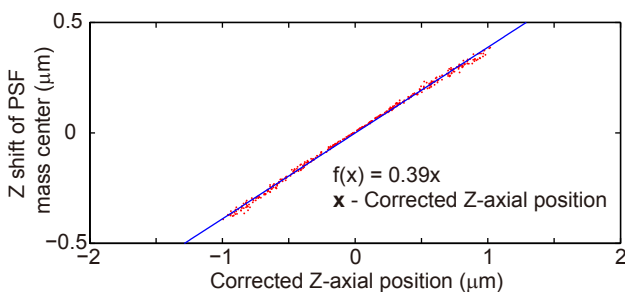
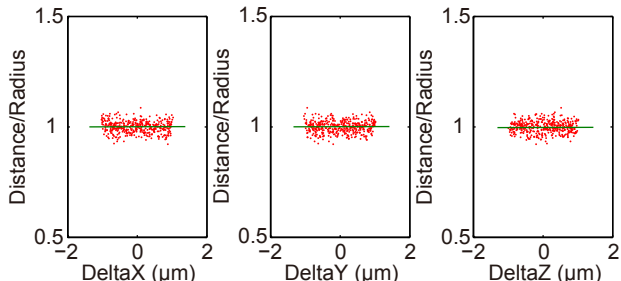
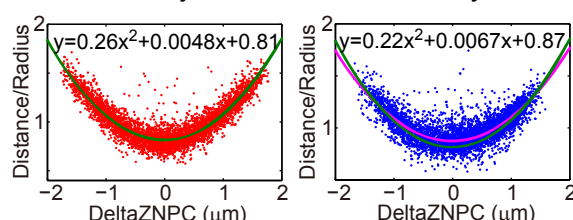
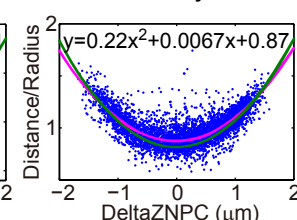
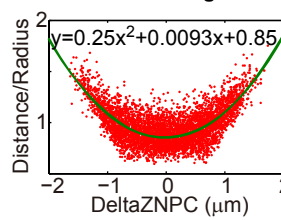
A**Sphere****B****Ellipsoid****C****Sphere simulation****D****Add simulated spherical aberration****E****Linear law****F****After correction****G****Normal objective****Silicon objective****Confocal laser scanning microscope**

Figure S1. Optical spherical aberration along the Z axis. **(A)** Normalized distances distribution of random spots on a sphere surface. **(B)** Normalized distances distribution of random spots on an ellipsoid surface ($R_z > R_x = R_y$, $R = (R_x + R_y + R_z)/3$). **(C)** Simulated normalized distances distribution of the spots on a sphere surface along the three dimensions (sphere radius is 1 μm ; the standard localization deviation of simulated spots is 0.03 μm). **(D)** Normalized distances distribution of spots on a sphere surface along the three dimensions with spherical aberration introducing linear distance overestimation along Z axis. **(E)** Using NPCs detection and approximation of the nucleus as a sphere, the overestimation along Z axis was measured. **(F)** Computed corrected position along Z axis. **(G)** The silicon immersion objective (left panel; Olympus; NA~1.35) decreased the aberrations compared to oil-immersion objective (right panel; Olympus; NA~1.4). **(H)** Spherical aberration along Z-axis using confocal laser scanning microscope.

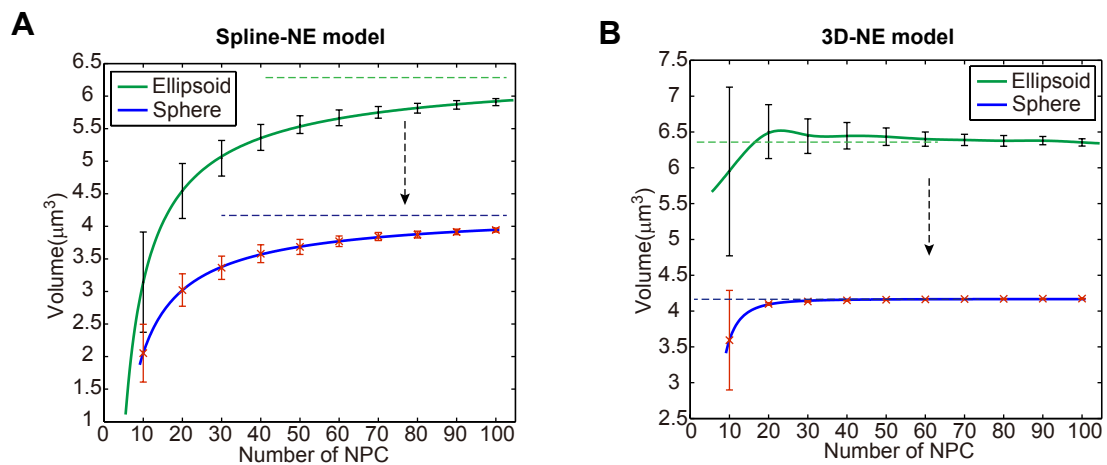


Figure S2. Evaluation of the spline-NE model and 3D-NE model. We simulated a sphere of radius=1 μm (volume=blue dashed line) and an ellipsoid (volume=green dashed line) of Rx=Ry=1 μm , Rz=1.5 μm . We calculated the volume of this sphere (blue line) or ellipsoid (green line) for different number of NPCs using either the spline NE-model (A) or the 3D-NE model (B), considering that the standard localization deviation of simulated NPCs is 0 μm .

Table S1. The volume of the nuclei along one cell cycle

t/min	0	15	30	45	60	75	90	105	120
Cell 1	3.92	4.26	4.52	4.71	5.11	3.57+1.69*	3.76+1.81*	4.22+2.12*	4.58+2.66*
					G2	End of mitosis			
Cell 2	4.14	4.11	4.13	4.67	5.26	5.08	3.82+1.78*	3.76+1.66*	4.05+1.73*
					G2	End of mitosis			
Cell 3	3.99	3.9	4.51	5.12	5.12	3.39+1.52*	3.54+1.55*	3.68+1.61*	4.11+1.89*
				G2	Anaphase				
Cell 4	2.99	3.4	3.9	4.1	3.83	2.98+0.81*	3.35+1.03*	3.55+1.29*	3.86+1.45*
					Anaphase				
Cell 5	3.29	3.5	3.59	3.76	3.91	4.23	3.11+1.76*	3.44+1.89*	3.16+1.87*
					G2				
Cell 6	2.95	3.38	3.57	4.07	4.34	2.9+1.87*	3.04+1.81*	3.22+2.01*	3.21+2.28*
					Anaphase				
Cell 7	3.2	3.42	3.71	3.71	4.92	4.88	3.23+1.56*	3.49+1.55*	3.21+1.92*
					G2	Anaphase			
Cell 8	4	4.02	2.49+1.57*	2.93+1.57*	3.19+1.82*	3.28+1.96*	3.24+1.63*	3.6	3.9
	G2	Anaphase							
Cell 9	3.91	3.99	4.1	5.53	5.1	3.09+1.99*	3.04+1.72*	3.51+2.35*	3.74+2.95*
				G2	Anaphase				
Cell 10	3.47	4.43	4.07	5.2	5.1	5.74	3.79+2.6*	3.8+2.63*	4.13+2.83*
					G2	Anaphase			

* represent the daughter nucleus.

Table S2. Summary nuclear and nucleolus size distribution in asynchronous cultures

Carbon source	NO. cells	Doubling time (min)	G1 percentage (%)	Median size of nucleus		V _{nucleolus} (μm ³)
				Surface (μm ²)	Volume (μm ³)	
Glucose	1054	90	42.2	10.99±1.36	3.41±0.60	1.38±1.15
Galactose	1061	120	45.4	9.77±1.16	2.83±0.50	0.82±0.82
Raffinose	1451	130	49.8	8.82±1.23	2.44±0.51	0.84±0.61
Ethanol	1116	220	71.1	6.84±1.15	1.66±0.41	0.29±0.21

Table S3: Genotypes of strains used in this study

Name	Genotype	Origin
BY4741	<i>MATA his3Δ1, leu2Δ0, met15Δ0, ura3Δ0</i>	(Brachmann et al., 1998)
W303-1a	<i>MATA, ade2-1, can1-100, his3-11,15, leu2-3,112, trp1-1, ura3-1</i>	(Thomas and Rothstein, 1989)
NOY1064	<i>MATA, leu2-3, 112, ura3-1, his3-1,1, trp1-1, ade2-1, can1-100, fob1Δ::HIS3</i>	(Cioci et al., 2003)
TMS1-1a	<i>MATA, his3-Δ1, leu2-Δ0, C, ura3-Δ0, ade2-801, lys2-801, LYS2::TETR-GFP, nup49-Δ::HPH-MX6, [pASZ11-NUPNOP: GFP-NUP49, mCherry-NOP1]</i>	(Albert et al., 2013)
Y24539	<i>MATA/MATA; ura3Δ0/ura3Δ0; leu2Δ0/leu2Δ0; his3Δ1/his3Δ1; met15Δ0/MET15; LYS2/lys2Δ0; NUP49/nup49::kanMX4</i>	Euroscarf
Y03254	<i>MATA, his3Δ1, leu2Δ0, met15Δ0, ura3Δ0, lys2Δ::KAN-MX4</i>	Euroscarf
YIL115c	<i>MATA, his3Δ1, leu2Δ0, met15Δ0, ura3Δ0, NUP159-TAP::HIS3</i>	GE-Dharmacon
3940	<i>MATA his3Δ1, leu2Δ0, met15Δ0, ura3Δ0, SPC42-GFP::HIS3</i>	(Huh et al., 2003)
3569	<i>MATA his3Δ1, leu2Δ0, met15Δ0, ura3Δ0, SPC42-mRFP::KANMX</i>	(Laporte et al., 2016)
Y15125	<i>MATAalpha, dyn1Δ::KAN-MX4, his3Δ1, leu2Δ0, lys2Δ0, ura3Δ0</i>	Euroscarf
yCNOD99-1a	<i>MATA his3-Δ1, leu2-Δ0, C, ura3-Δ0, ade2-801, lys2-801, lys2-Δ::KAN-MX, nup49Δ::HPH-MX6 [pASZ11-NUPNOP: GFP-NUP49, mCherry-NOP1]</i>	This work
yRW3-1a	<i>MATA leu2-3, 112, ura3-1, his3-1,1, trp1-1, ade2-1, can1-100, fob1Δ::HIS3, NUP57-tDimerRFP::LEU2 [pASZ11-GFP-NUP49]</i>	This work
yRW4-1a	<i>MATA, leu2-3, 112, ura3-1, his3-1,1, trp1-1, ade2-1, can1-100, fob1Δ::HIS3, NUP2-tDimerRFP::URA3 [pUN100-GFP-NUP49]</i>	This work
yRW5-1a	<i>MATA his3Δ1 leu2Δ0 met15Δ0 ura3Δ0, NUP159-GFP::klURA3</i>	This work
yRW6-1a	<i>MATA his3Δ1 leu2Δ0 met15Δ0 ura3Δ0, NUP159-GFP::HIS3</i>	This work
yRW7-1a	<i>MATA his3Δ1 leu2Δ0 met15Δ0 ura3Δ0, NUP159-GFP::HIS3, NUP2-tDimerRFP::URA3</i>	This work
yRW8-1a	<i>MATA his3Δ1 leu2Δ0 met15Δ0 ura3Δ0, NUP159-GFP::klURA3, NUP57-tDimerRFP::LEU2</i>	This work
yRW9-1a	<i>MATA, his3Δ1, leu2Δ0, met15Δ0, ura3Δ0, SPC42-mRFP::KANMX, [pUN100-GFP-NUP49]</i>	This work
yRW10-1a	<i>MATA, his3Δ1, leu2Δ0, met15Δ0, ura3Δ0, SPC42-GFP::HIS3, NUP57-tDimerRFP::LEU2</i>	This work
yRW11-1a	<i>MATA, his3-Δ1, leu2-Δ0, C, ura3-Δ0, ade2-801, lys2Δ::KAN-MX, nup49Δ::HPH-MX6, SPC42-GFP::HIS3 [pASZ11-NUPNOP: GFP-NUP49, mCherry-NOP1]</i>	This work
yRW19-1a	<i>MATA, his3-Δ1, leu2-Δ0, C, ura3-Δ0, ade2-801, lys2-801, lys2Δ::NAT-MX4, nup49Δ::HPH-MX6, dyn1Δ::KAN-MX4 [pASZ11-NUPNOP: GFP-NUP49, mCherry-NOP1]</i>	This work
yRW20-1a	<i>MATA, his3-Δ1, leu2-Δ0, C, ura3-Δ0, ade2-801, lys2-801, lys2Δ::NAT-MX4, nup49Δ::HPH-MX6, SPC42-GFP-HIS3, dyn1Δ::KAN-MX [pASZ11-NUPNOP: GFP-NUP49, mCherry-NOP1]</i>	This work
yCNOD203-1a	<i>MATA, ade2-1, can1-100, his3-11,15, leu2-3,112, trp1-1, ura3-1, nup49-Δ::KAN-MX, BIM1::URA3::BIM1-tDimerRFP [pASZ11-GFP-NUP49]</i>	This work

Table S4: Plasmids used in this study

Name	Author/Reference
pUN100-GFP-NUP49	(Wimmer et al., 1992)
pFA6-GFP-HIS3	(Longtine et al., 1998)
pASZ11-GFP-Nup49	(Siniossoglou et al., 2000)
pFA6a-GFP(S65T)-KIURA3	(Sung et al., 2008)
pRS306-NUP2-tDimerRFP	(Laporte et al., 2016)
pBIM1-tDimerRFP	(Laporte et al., 2016)
pRS305-NUP57-tDimerRFP	This work

References

- Albert, B., Mathon, J., Shukla, A., Saad, H., Normand, C., Leger-Silvestre, I., Villa, D., Kamgoue, A., Mozziconacci, J., Wong, H. et al.** (2013). Systematic characterization of the conformation and dynamics of budding yeast chromosome XII. *J Cell Biol* **202**, 201-10.
- Brachmann, C. B., Davies, A., Cost, G. J., Caputo, E., Li, J., Hieter, P. and Boeke, J. D.** (1998). Designer deletion strains derived from *Saccharomyces cerevisiae* S288C: a useful set of strains and plasmids for PCR-mediated gene disruption and other applications. *Yeast* **14**, 115-32.
- Cioci, F., Vu, L., Eliason, K., Oakes, M., Siddiqi, I. N. and Nomura, M.** (2003). Silencing in yeast rDNA chromatin: reciprocal relationship in gene expression between RNA polymerase I and II. *Mol Cell* **12**, 135-45.
- Huh, W. K., Falvo, J. V., Gerke, L. C., Carroll, A. S., Howson, R. W., Weissman, J. S. and O'Shea, E. K.** (2003). Global analysis of protein localization in budding yeast. *Nature* **425**, 686-91.
- Laporte, D., Courtout, F., Tollis, S. and Sagot, I.** (2016). Quiescent *Saccharomyces cerevisiae* forms telomere hyperclusters at the nuclear membrane vicinity through a multifaceted mechanism involving Esc1, the Sir complex, and chromatin condensation. *Mol Biol Cell* **27**, 1875-84.
- Longtine, M. S., McKenzie, A., 3rd, Demarini, D. J., Shah, N. G., Wach, A., Brachat, A., Philippsen, P. and Pringle, J. R.** (1998). Additional modules for versatile and economical PCR-based gene deletion and modification in *Saccharomyces cerevisiae*. *Yeast* **14**, 953-61.
- Siniossoglou, S., Lutzmann, M., Santos-Rosa, H., Leonard, K., Mueller, S., Aeby, U. and Hurt, E.** (2000). Structure and assembly of the Nup84p complex. *J Cell Biol* **149**, 41-54.
- Sung, M. K., Ha, C. W. and Huh, W. K.** (2008). A vector system for efficient and economical switching of C-terminal epitope tags in *Saccharomyces cerevisiae*. *Yeast* **25**, 301-11.
- Thomas, B. J. and Rothstein, R.** (1989). Elevated recombination rates in transcriptionally active DNA. *Cell* **56**, 619-30.
- Wimmer, C., Doye, V., Grandi, P., Nehrbass, U. and Hurt, E. C.** (1992). A new subclass of nucleoporins that functionally interact with nuclear pore protein NSP1. *Embo J* **11**, 5051-61.